Reviews in Mineralogy & Geochemistry
Vol. 57, pp. 435-448, 2005
Copyright © Mineralogical Society of America

Micro- and Mesoporous Carbon Forms, Chrysotile, and Clathrates

Marcello Mellini
Dipartimento di Scienze della Terra
Via Laterina 8
53100 Siena, Italy
mellini@unisi.it

INTRODUCTION

This chapter offers a not-exhaustive overview of structural mesoporosity in selected, natural mineral phases (carbon forms, chrysotile, gas hydrates). After a short introduction devoted to the introduction of the most general features of porosity, attention will be paid mostly to natural mesoporous mineral phases, leaving microporosity to other chapters of this volume. However, a few peculiar microporous structures will be also considered, because of their close resemblance with the mesoporous substances.

Conversely, no attempt will be made to report properties and structures of the many examples of man-made mesoporous materials including silica xerogels, mesoporous synthetic silica, calcium phosphate and the fantastic arrangements of shapes, surface patterns and channels that can occur (e.g., Yang et al. 1997; Maschmeyer 1998; Sayari 2003; Xia et al. 2003; Zheng et al. 2003; White et al. 2005). Similarly, the overview will not deal with crystal engineering processes, such as the fabrication of hollow porous shells of calcium carbonate from self-organizing media (oil-water-surfactant microemulsions supersaturated with calcium carbonate; Walsh and Mann 1995). Finally, one more aspect outside the scope of this article will be micro-to-mesoporosity conversion in synthetic materials, such as activated palygorskite and sepiolite, or the so-called pillared clays (e.g., Mass et al. 1997; Dékany et al. 1999; Salerno and Mendioroz 2002; Ferraris and Gula 2005). Evidently, these issues represent extremely important technological targets, often achieved following synthetic routes that may be totally different from those used by nature to form minerals.

Microporosity, mesoporosity and macroporosity

Pore size. Porous structures are derived from a framework of linked atoms ("host"), that create volumetrically important voids ("pores"), possibly capable of including several different "guest" species. Three groups (micro-, meso- and macropores) are discriminated based upon pore size. According to International Union for Pure and Applied Chemistry (IUPAC) recommendations, pores with free diameters less than 2 nm should be called micropores (McCusker et al. 2001, 2003; McCusker 2005). Pores in the 2–50 nm range are mesopores while pores larger than 50 nm are characterized as macroporous materials. Ideally, pores repeat in a regular manner, forming long-range ordered structures; otherwise, the material may be non-crystalline, even if other kinds of short-range or long-range order are present (e.g., in the internal structure of the pores, or the manner in which adjacent pores come together, respectively). A systematic nomenclature of porous structures, as well as criteria for obtaining comprehensive crystal-chemical formulae that reflect the chemical composition of host and guest, structures of host and pores, symmetry, atom connectivity and pore dimensionality may be found in McCusker et al. (2001, 2003).

1529-6466/05/0057-0012$05.00 DOI: 10.2138/rmg.2005.57.12

Synthetic micro- to macroporous structures. Interest in micro- and mesoporous materials arises from the important technological properties that these materials possess. For instance, Zheng et al. (2003) reported the synthesis of a series of microporous, three-dimensional open-framework sulfides and selenides, containing highly mobile alkali metal cations, exhibiting fast-ion conduction with potential applications in devices such as batteries, fuel cells, photocatalysts and electrochemicals sensors.

As regards mesoporous materials, their possible uses are simply extraordinary, ranging over catalysis, oxidation, hydrogenation, halogenation, polymerization, and membranes and offering unique electronic, magnetic and optical properties (Maschmeyer 1998 and references therein). One more important feature derives from the development of synthetic routes leading to derivatized products tailored for particular chemical aims, through fine-tuning of structure, composition and physical properties (e.g., Sayari 2003). Consequently, mesoporous materials are actively studied within the framework of so-called "green chemistry," that focuses on replacement of resource- and energy-demanding chemical routes by environmentally friendly catalytic methods. Also from the point of view of basic science, the mesoporous world offers exciting perspectives, being intimately linked with topics such as self-assembled structures and spontaneous patterning (e.g., Aizenberg et al. 1999). Last but not least, the need to deal with the nanoworld of mesoporous phases is leading to advanced investigation techniques, such as electron microscopy imaging (e.g., Sakamoto et al. 2003) and non-trivial applications of X-ray powder diffraction and spectroscopies (electron-spin resonance, Raman, NMR, EXAFS, UV-Vis).

In some cases, technological exploitation has been inspired by the study of natural materials. For instance, opal is a natural silica form, characterized by mesoporous arrangements (Graetsch 1994). In particular, precious opal is a non-crystalline material, with $SiO_2 \cdot nH_2O$ chemical composition, consisting of close-packed homometric spheres of amorphous silica, usually 150–350 nm in diameter (Rossman 1994). Diffraction effects originate because each sphere has diameter close to the visible light wavelength; depending upon the actual size of the amorphous spheres and stone orientation, with iridescence leading to the well-known play of color in opal. Packing of spheres necessarily leaves some open space as interstices and voids with sizes that depend on sphere diameter. However, detailed determination of water content and specific surface area reveals values lower than expected, consistent with the presence of intersphere cement that partially clogs the ideal close-packing of rigid spheres. This feature is immediately evident in scanning electron microscope images as sphere coalescence or partial polygonalization. Distinct from monodispersed precious opals, non precious opals (*"potch opals"*) fail to show optical diffraction effects, because they are formed by irregular packing of polydispersed heterometric spheres (Gauthier et al. 1995). Both diffracting and non-diffracting opals may be stained to different colors by mineral pigments (hematite, red; copper minerals, blue) as pore-fillers.

After 1992, an explosion in the study of mesoporous silica led to over 3000 papers (Sayari 2003), dealing with three main mesophases (MCM-41, hexagonal; MCM-48, cubic; MCM-50, lamellar). These are often synthesized by supramolecular templating, using long chain alkyltrimethilammonium surfactants whose electrostatic interaction triggers a self-assembly process that controls the nature of the final mesophase; other surfactants lead to different silica mesophases including SBA-1 to SBA-16, MSU-n, MSU-V, MSU-G, HMS (Firouzi et al. 1995). Varying the synthesis conditions produces silica mesophases of varying morphologies. Thin films, spheres, fibers and monoliths are the simplest shapes; otherwise, particles with spiral, discoidal, toroidal, pinwheel, doughnut and other exotic shapes have been reported. Mesostructured chalcogenides and mixed oxides further increase the chemical, structural and morphological diversity of synthetic materials. According to Sayari (2003), the amount of

information is now so large as to frustrate any attempt to write a book-sized, comprehensive review on periodic mesoporous materials.

Spherical colloids have been used as versatile templates, capable of generating macroporous phases (Xia et al. 2003). In this method, the voids in the colloidal crystal resulting from regular sphere packing are infiltrated with a precursor solution or gel. Finally, chemical removal of the sacrificial template produces three-dimensional macroporous materials with interesting bandgap properties ("photonic" crystals), and potential application in fields such as filtration, separation and purification. Sometimes, these materials are referred to as inverted, or inverse, opals.

Finally, one more stimulating research topic, at least in part connected with porosity, can be drawn from the nanowire world. Nanowires (often named as "quantum wires" by physicists) are anisotropic nanocrystals of extreme length/diameter ratio (Yan and Yang 2003). Their technological importance derives from exceptional properties, such as mechanic toughness, photoluminescent efficiency, thermoelectric behavior, nonlinear optical behavior, and low lasing threshold.

Structural constraints. More than a mere classification issue, the distinction among micro-, meso- and macropores perhaps masks a very important issue, associated with different types of particle interactions. Namely, it is crucial to understand what forces actually control porosity development. I tentatively propose here some schematic guesses, with the aim to verify their validity by the details reported in the following paragraphs.

Possibly, void development may be controlled i) by strong, first-neighbor atom-atom bonds in microporous systems; ii) by weak intraparticle non-bonding interactions in mesoporous systems; or iii) by particle coalescence in macroporous systems.

Furthermore, voids may arise from a combination of intrinsic and extrinsic factors. One intrinsic reason for porosity development would be a strongly anisotropic shape of the building particle; namely, internally strong bonded units pack together leaving open-space, as observed in the partially empty rod-close packing of chrysotile (e.g., Mellini 1986). Examples for extrinsic control may be found in the reaction environment, for instance in terms of outer anisotropic fields (*e.g.*, tectonic shear strain) that impose orienting forces capable of controlling void shape.

Finally, a still open problem deserving consideration is connected with the appraisal of the self-assembly mechanisms operative in micropatterned mesoporous systems. In particular, an extremely exciting perspective are biotic-abiotic, organic-inorganic interactions in biomineralization processes (Banfield and Nealson 1997; Dove et al. 2003).

Mesoscale and Earth Sciences. From the point of view of Earth Sciences (Baronnet and Belluso 2002), synthetic nanostructured meso- and macroporous materials are worthy of study as they offer insights into the origin of shape complexity in the mineral kingdom (e.g., in terms of mineralization processes, their intensive P and T parameters, the role of catalytic species, and the effects of dilute chemical components that may not immediately appear within the crystallization reaction). As already anticipated, even more complex and interesting effects are found in moving from totally inorganic mineral to biomineral systems (McLean et al. 2001; Dove et al. 2003), or to the interactions between minerals and microbes (Banfield and Nealson 1997). Here, templating effects are required to quantitatively explain the crystallization of phases far from their stability field (e.g., deposition of calcium carbonate as the high-pressure polymorph, aragonite, within a shell living at low-pressure, in a shallow level of the coral reef).

CARBON FORMS

Basically, the low-pressure forms of carbon are based upon the graphene sheet structure, namely upon a six-membered carbon sheet, that can be folded and rolled to yield different carbon forms (Buseck 2002).

Anthracite

Anthracite offers several examples of externally-controlled porous arrangements of carbon, with the final pore size determined by metamorphic and tectonic shear stresses. This mineral has been long known to be microporous, with pores flattened parallel to the bedding by pressure yielding a long-range statistical preferred orientation (Bonijoly et al. 1982), that results in anisotropic texture and biperiodic turbostratic crystallization. Mesopores, and even macropores, can evolve with the changing conditions. For instance, meta-anthracite differs from anthracite only by the increasing coalescence of adjacent pores. Semi-graphites are formed by single macropores, occurring as hollow distorted polyhedral shells (Bonijoly et al. 1982). Finally, increasing P, T and shear stress destroys porosity, with lamellar graphite representing the limit of a flattened macropore. More recently, evolution of carbonaceous material to graphite in a high-pressure, low-temperature metamorphic environment has been studied in detail by Beyssac et al. (1994), who describe micropores and onion-ring-like phases, preferentially transforming to graphite in the outer ring, namely in the areas with the highest radius of curvature.

While the carbon structure is difficult to study, even using accurate local probes such as HRTEM, detailed information is important for understanding the behavior of coal char during combustion or gasification. Therefore, the need to deal quantitatively with the char structure has led to the development of HRTEM filtering techniques, that generate numerical information concerning graphene layer size, interlayer spacing, the number of layers per stack, and their textural distribution (Sharma et al. 1999). From such studies (e.g., Rouzaud and Clinard 2002) it has been shown that carbon materials offer multiscale organization from the subnanometric to the millimetric scale, whose formation is determined by synthesis conditions, that results in a variety of industrially important chemical and physical properties.

In the recent years, carbon research has focused on two specific forms, nanotubes and fullerenes.

Carbon nanotubes

Carbon nanotubes have been extensively investigated, beginning with the first images reported by Iijima (1991). In fact, their hollow cores, coupled with large aspect ratio, make them candidates for a host of nanotechnological applications. Synthetic carbon nanotubes have interesting porosity, that may be modulated according to the specific need. For instance, it is possible to grow carbon nanotubes with controlled inner diameter, from 4.3 ± 2.3 nm, or definitely larger. These tubes may adopt a strongly oriented pattern, forming membranes with tailored transport properties. By filling nanotubes with metal, composite nanodevices are created consisting of a metal nanowire surrounded by a dielectric shield (Ajayan and Iijima 1993). Finally, carbon nanotubes are expected to behave as tough nanomanipulators, suitable as nanoscale mass conveyors (e.g., Regan et al. 2004). Notwithstanding their apparent resemblance with chrysotile nanotubes (see later), carbon nanotubes of natural origin have not yet been reported.

Carbon nanotubes may be considered as modifications of the basic sp^2 carbon graphite sheet, that due to the absence of strong three-dimensional chemical bonding may be rolled into tubes while conserving the six-membered carbon rings.

Fullerenes

Alternatively, the carbon sheet may be further modified, possibly by introduction of sp^3 defects (Hiura et al. 1994), to achieve a different connectivities. In particular, a few of the six-membered rings may become five-membered (pentagons), obliging the sheet to form large molecules arranged in closed surfaces ("soccer balls") with truncated icosahedron shape and C_{60} (or C_{70}, C_{76} and C_{84}) chemical compositions. These cage-like molecules, named fullerenes, may be synthesized in large amounts, by passing an electric current between two graphite electrodes, under helium (e.g., Ball 2001). Also in the case of fullerenes, several potential applications have been proposed and investigated, with variable success (superlubricants, superconductors, exceptionally stiff materials).

Whatever the future applications of synthetic fullerenes and nanotubes, they have already activated a huge amount of research. Therefore, it seems appropriate to spend a few words about the possible natural occurrences of these exotic carbon forms.

Following the synthesis of fullerenes by Kroto et al. (1985), it was not until 1992 that their first natural occurrences were reported as thin films within fractures in a carbon-rich rock from Karelia, named shungite (Buseck et al. 1992). In the same year, C_{60} and C_{70} fullerenes were also extracted directly from coal by chromatography (Wilson et al. 1992) and from a fulgurite (Daly et al. 1993). A few years later, fullerene-like carbon nanostructures were found also in the Allende carbonaceous-chondritic meteorite (Harris et al. 2000), as closed nanoparticles 2–10 nm in diameter, supposedly capable behaving as carriers of primordial planetary gases in the extraterrestrial space.

Notwithstanding the large excitement arising after those discoveries natural occurrences may be rare, and many unresolved questions remain about the identity and formation of fullerenes in geological environments (Buseck 2002, and references therein).

SERPENTINE

Chrysotile mesopores

Among the different serpentine minerals—the flat-layer lizardite, the polygonally-shaped polygonal serpentine, the corrugated-layer antigorite, and the curled-layer chrysotile; (Wicks and O'Hanley 1989)—it is the last that offers the most interesting mesoporosity properties. Historically, one of the first successful mineralogical applications of electron microscopy was the demonstration that "both natural and synthetic chrysotile crystallize in the form of hollow cylindrical tubes" (Bates et al. 1950; Noll and Kirchner 1950). Although quite short, that early report captured other features common for chrysotile, namely the "uniform diameter" of several hundreds Å, the presence of multiple tubes and "the interesting conical development of the tubes." The hollow-tube model was further investigated by Pundsack (1955, 1956, 1961), who investigated in detail the colloidal behavior of the chrysotile suspensions, including its surface chemistry, density and structure. Basically, Pundsack questioned the hollow-tube model, by postulating that only a limited volume was actually void. In particular, density measurements suggested a maximum void volume of 6%, rather than the 20–30% expected for the fiber bundle. Therefore, Pundsack (1955 and 1956) was obliged to postulate that "distorted strips or ribbons of fibers rather than …hollow tubes" were present, and to conclude that "the sample viewed in the electron microscope no longer bears a one to one relationship with the native fiber." In any case, not all the porosity of the hollow-tube model was actually available for nitrogen adsorption, for reasons then unknown. Finally, Pundsack (1961) concluded on the basis of adsorption-desorption isotherms that 80% of the observed void volume existed in pores less than 60 Å in diameter, that the cylindrical chrysotile fibers

have average outer diameters of 200–250 Å and average inner diameters of 20–50 Å, and that interfibril space was irregular but with an effective pore size similar to the intrafibril pores. In a contemporaneous electron microscope study, Bates and Comer (1959) proposed that the tubes contain amorphous material with chrysotile-like composition. Using X-ray diffraction, Whittaker (1957) suggested that the hollow tubes were filled with curved laths of the same composition as the tubes themselves, and that this material should be amorphous, as indicated by contrast analysis (Whittaker 1966). Similarly, Martinez and Comer (1964) supported the presence of amorphous interfiber material, after extracting the material by ultrasonic treatment of chrysotile crudes.

The partially-filled model of Pundsack was however, at least in part, refuted by Huggins and Shell (1965). These authors also reported extensive data in favor of the existence of totally hollow tubes. More recently, the pioneer high resolution TEM work of Yada (1967 and 1971) apparently supported the predominantly hollow-tube model, concluding that the central hollow was most frequently 70–80 Å in diameter, that the outer diameter of the fiber was 220–270 Å and that the wall had constant thickness of up to 100 Å (Fig. 1). Comparison of subsequent TEM investigations indicates that the actual values are specimen-dependent, as different occurrences lead to slightly different sizes. In any case, it is now confirmed, that from 350 Å diameter, further growth of chrysotile leads to non-porous polygonal shapes (Mellini 1986; Baronnet et al. 1994).

Pore-dependent properties

The variable porosity of the chrysotile fiber bundles suggests that this property may be specimen-dependent, as well as treatment-dependent. This point was first addressed by Naumann and Dresher (1966) in a study dedicated to the influence of sample texture on chrysotile dehydroxylation. The higher the surface area of chrysotile, the faster its thermal transition to an intermediate amorphous phase, and subsequent crystallization as olivine. Therefore, at that time it was already clear that differently textured chrysotiles might exist, that they might vary in the amount of interstitial material, that the actual amount of void space had an important bearing on dehydroxylation kinetics, and that chrysotile samples from different sources might display different porosity-related properties.

Subsequently, the issue of porosity and reaction kinetics became important in view of the technological utilization of chrysotile (e.g., Monkman 1971; Choi and Smith 1972; Atkinson 1973; Bleiman and Mercier 1975), in addition to the health hazard possibly arising from chrysotile inhalation (as a result of interaction with physiological fluids) and its influence on water dissolution reactions within groundwater systems at landfill sites (Gronow 1987; Tartaj et al. 2000). Basically, these studies demonstrated acidic decomposition of chrysotile, through the breakdown of fiber-bundles into individual fibrils (simultaneous with the release and/or reaction of the interfibrillar material), and by migration of ions along the tube. Magnesium cations appeared continuously released from the fibers, in a manner not unlike magnesium hydroxide (Pundsack and Reimschussel 1956) leaving a silica skeleton that preserved the primitive fiber shape. As the rate limiting factor was the acidic removal of the basic brucite layer from the fiber surface, the smaller the particle size the faster the reaction.

Increasing interest in the adsorption properties of chrysotile, and of leached chrysotile, led to comparative analyses of several specimens. For example, Suquet (1989) reported sharply different adsorption properties in different samples of chrysotile. For instance, one of them adsorbed twelve times less phenantrene and 45% less CO_2 than the other. Furthermore, chrysotile adsorption properties were dependent on preparation; in fact, dry grinding converts the long fibers into shapeless, non crystalline material, with strongly active basic sites, that can adsorb CO_2 and H_2O directly from the atmosphere (Suquet 1989). Titulaer et al (1993)

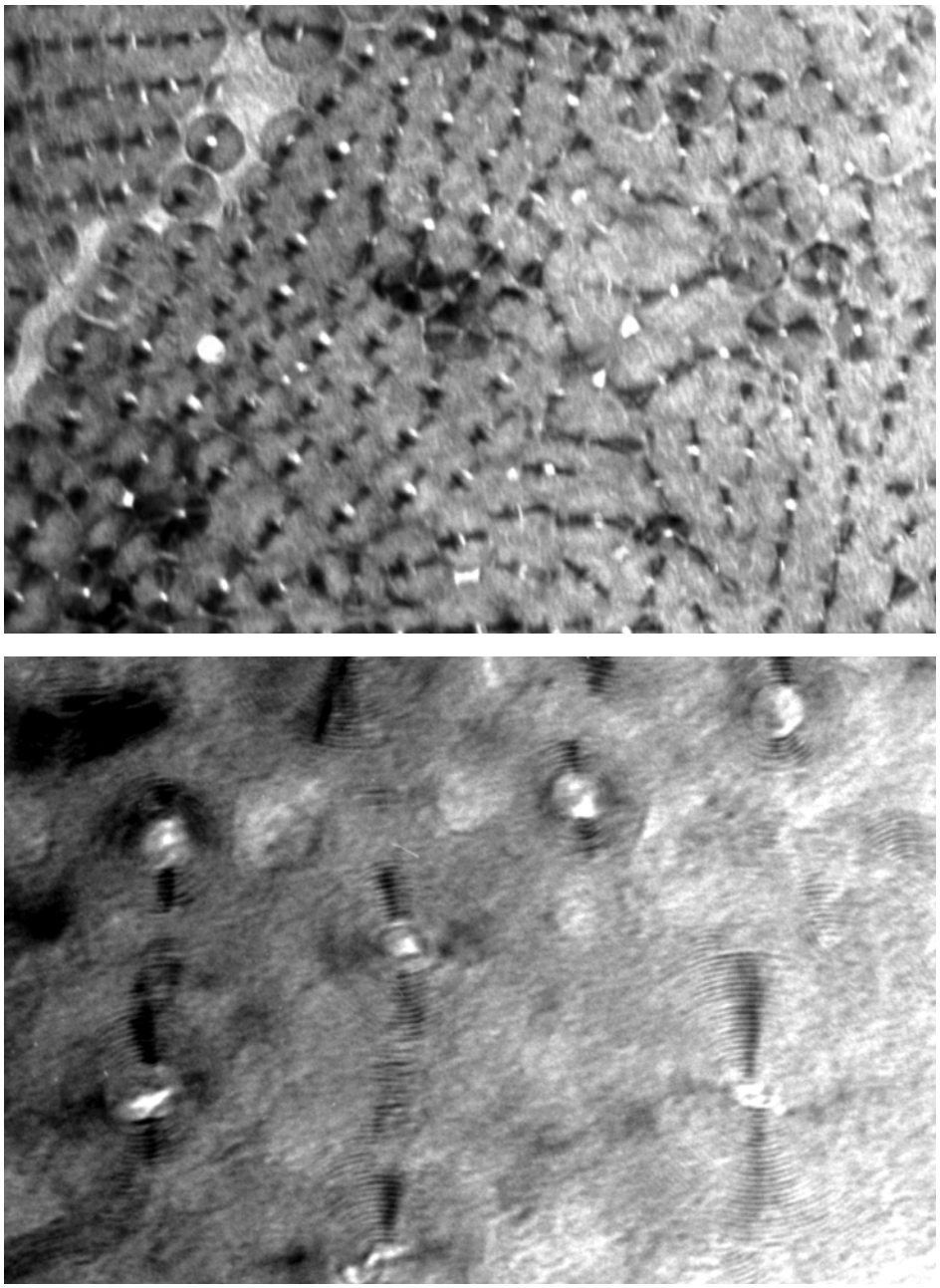

Figure 1. (*top*) Rod close-packing of chrysotile fibers, as seen along the fiber axis (ion-thinned section). Average diameter of the fiber close to 300 Å. Pores appear as low contrast regions, in the center of the individual fiber and at the junctions among three adjacent fibers. (*bottom*) Enlarged view of the chrysotile rod-close packing, showing bent (001) layers, deformed central holes and poorly crystalline interfiber filling.

applied diffuse reflectance infrared spectroscopy (DRIFTS), extended sorption studies using nitrogen, and performed thermoporometric characterization to determine values of 50-80 Å for the hollow-tube inner diameter, and of 36–46 Å for the diameter of the channel running among clustered tubes. These results were in good agreement with pre-existing and their own TEM determinations.

An interesting application of adsorption in mesoporous chrysotile was presented by Soma et al. (1993), with the aim to enhance optical chrysotile recognition during environmental monitoring. They used fluorescent xanthene dyes with carboxyl or hydroxyl groups to mark chrysotile, to exploit the preferential adsorption of basic dyes in chrysotile, with respect to kaolinite, gypsum, sulfur and glass wool. In particular, calcein and umbelliferone appeared to be suitable dyes for selective detection of chrysotile by fluorescence microscopy. The same monitoring issue was also theoretically approached by Balan et al. (2002); they observed multiple ionic-plasmon resonance in the IR-spectra of chrysotile nanotubes, and modeled these IR effects to calculate the geometrical parameters of nanotube based materials.

The origin of pores in chrysotile

The porosity of chrysotile therefore depends upon the configuration of the tetrahedral-octahedral 1:1 layer, the organization into cylindrical or spirally wrapped tubes, the rod-close packing of strongly textured chrysotile fiber-bundles, and the empty space resulting from poorly textured arrangements. Following Yada and Iishi (1977) we know that the morphological and structural features of synthetic chrysotile are controlled by reaction parameters such as pH, time and temperature. To summarize, early formed nuclei consist of membranes a few unit cells thick, laterally extending for several hundred Angstroms. Within 30 minutes at 300–400°C, these quickly curl into cylindrical or conical shapes. So, in absence of strong three-dimensional chemical bonds, internal tensions lead to wrapping of the serpentine membrane, and the resultant curled shapes.

The chrysotile growth process has been further studied in detail by Baronnet and Devouard (1996), and Amelinckx et al. (1996). In both cases the growth of chrysotile was analyzed in terms of elastic strain and departure from equilibrium, and ultimately the formation of 15- and 30-sector fan-like arrangements of flat lizardite sectors.

In the assessment of the present author, it is evident that chrysotile is an open structure with 5–30% void space. As nature will circumvent void formation if possible (*"horridum vacui"*), transition from open-space chrysotile to fan-shaped polygonal serpentine represents an effective space-saving system. In other words, it is to be expected that chrysotile will be favored under extensional regimes (e.g., Andreani et al. 2004), and polygonal serpentine under compressive regimes.

More water than space?

Retrograde serpentinites often consist of meshes, formed by replacement of olivine. Whereas the mesh rim is mostly formed by oriented, non-topotactic lizardite (Rumori et al. 2004), the mesh core consists of a chaotic mixture of lizardite flakes, polygonal serpentine sectors, chrysotile fibers and more-or-less amorphous material (Viti and Mellini 1998). The variable amount and distribution of magnetite leads to the dark color of serpentinites; in particular, the darker varieties have been extensively used as decorative stones for at least twenty centuries, as in the Romanic and Gothic churches of Tuscany that are often adorned by alternating strips of white marbles and dark-green serpentinites.

During a study on serpentinite alteration, Bralia et al. (1995) systematically measured anomalous water saturation indices. This parameter measures the percentage of pores accessible to water diffusion, with respect to the whole porosity determined using helium

diffusion. The values were 131 and 161%, for weathered stones extracted from the Siena Cathedral and from altered quarry surfaces, respectively. Therefore, unlike other stones, the quantity of pores accessible to water was >100%, indicating that water diffuses through serpentinites more easily than the helium gas used for rock porosity determination (close to 4–5%). In other words, the amount of water entering the serpentinite was greater than the available space. This anomaly was interpreted as due to the presence of inaccessible, sealed pores within the complex serpentinite texture; excess water uptake was due to permeability through pre-existing soluble barriers, that prevented gas flow into the sealed pore-space. The barrier material was thought to be akin to the brucite-depleted $MgSi_2O_5$ residue envisaged by Pundsack (1956) and Suquet (1989), possibly formed by weathering processes acting on very short time scales, as demonstrated by the normal water saturation indices of very fresh specimens.

Serpentine mesopores: from gas carriers to nanowires templates

Serpentine porosity may offer exciting perspectives also under certain extreme scenarios in the primitive Solar System and the deep ocean floor. In the first case, primitive meteorites like the Cold Bokkeveld or the Mighei CM carbonaceous chondrites are rich in serpentine nanotubes, formed by aqueous alteration prior to the arrival on Earth (Zega and Buseck 2003; Zega et al. 2004). As noted by these authors, an intriguing possibility is that the silicate nanotubes could have served as carriers of primordial fluids. The other scenario is connected with present-day ocean floors, and the continuous release of hydrocarbons abiotically formed during the peridotite serpentinization; we may wonder whether the serpentine micropores could behave as methane traps to control methane transfer from the lithosphere to the ocean, possibly interacting with gas hydrates in the global carbon budget.

Chrysotile nanotubes have also been studied as nanowires templates (Grobéty et al. 2004). By filling the hollow-tube of chrysotile by appropriate metals, it would be possible to obtain a composite material having a tiny conducting core surrounded by a dielectric silicate wall. Apparently, this property was recognized as early as in 1960 by Cosslett and Horne (1960). They modified the TEM contrast of chrysotile from light to dark fibril core, by filling it by potassium phosphotungstate; the experiment was repeated by Clifton et al. (1966), introducing lead nitrate and decomposing *in situ* to lead oxide.

Finally, mesopores with average diameter of 20 Å diameter have been obtained by acid treatment of antigorite (Kosuge et al. 1995). If successful, this approach might lead to substitutes that would comply with current regulations limiting the use of chrysotile fibers.

CLATHRATES

Enclosure compounds

Clathrates are non-stoichiometric enclosure compounds, formed by combining two stable compounds, with no chemical bond between the two components (Sloan 1998). One of them (the host) forms a cage-defining three-dimensional frame; the other component (the guest) is physically trapped within the cages and stabilizes the clathrate, that would not exist without the trapped guest. In Earth Sciences gas hydrates represent the most significant class of clathrates. The most important is methane hydrate, with end-member composition of $CH_4 \cdot 5.76H_2O$ in the case of completely occupied cages. Although quite paradoxical, no gas hydrate has ever been recognized as an accepted mineral species.

Physically, gas hydrates look like ordinary water ice, from which they differ in the larger density value of 0.95 g/cm^3 as compared to ~0.92 g/cm^3. From the structural point

of view, gas hydrates (known as clathrate hydrates as well) present three different crystal structures. The most common ones are cubic (structure I, *Pm*3*n*, *a* = 12 Å; structure II, *Fd*3*m*, *a* = 17.3 Å); they are stabilized by guest gases ranging in size from argon to *p*-dioxane (i.e., diameters 3.8–6.8 Å). The third phase (hexagonal *P*6/*mmm*, *a* = 12.26, *c* = 10.17 Å) can host still larger molecules (e.g., methylciclohexane or hexacloroethane; Ripmeester et al. 1987). As the diameter of the cavities range from 7.8 to 9.2 Å, the upper limit for the stability of gas hydrates is assured by molecular diameters up to 9 Å and therefore these compounds are more properly included in the microporous group. The basic cage of gas hydrates is a pentagonal dodecahedron, consisting of twelve pentagonal faces, often indicated as 5^{12}. As dodecahedra alone cannot fill space, polyhedral packing is completed with tetrakaidecahedra $5^{12}6^2$, namely polyhedra with twelve pentagonal and two hexagonal faces. Two 5^{12} and six $5^{12}6^2$ cages, linked together through vertices, form the so-called structure I. Structure II still contains sixteen $5^{12}6^2$ cages, linked to eight hexakaidecahedra (12 pentagonal and 6 hexagonal faces), that meet by face sharing (Englezos 1993, and references therein). Finally, structure III is based upon two 5^{12} cages, one $4^35^66^3$ cage, and a very large $5^{12}6^8$ cage (Ripmeester et al. 1987). Comprehensive reviews of structure and properties of gas hydrates may be found in Sloan (2003a,b), and more recently, almost a whole issue of American Mineralogist has been dedicated to this topic (Sloan 2004, and companion papers).

Quite interesting, natural gas hydrates develop a complex porosity, because they contain both the micropores deriving from their constituent cages, as well as larger eso- and macropores, usually ranging from 100 to 500 nm and occasionally reaching 1 μm (Kuhs et al. 2000, 2004).

Owing to their peculiar nature, the study of gas hydrates requires an approach based upon specific techniques (Sloan 2003b; Genov et al. 2004). The most frequently used have been X-ray powder diffraction (e.g., used to test the possible structural models); solid-state nuclear magnetic resonance (to support the structure models and to determine the absolute occupancy cages by the gas); Raman spectroscopy (to determine the environment of hydrate guests); electron microscopies and finally, theoretical modeling.

Energy resource and/or geological hazard

Negative aspects of gas hydrates are well known, as they may lead to the obstruction of natural gas pipelines in cold regions unless expensive nucleation inhibitors are used. However, starting from 1990 (e.g., Englezos 1993), gas hydrates attracted interest, because of their possible economic and environmental importance (Haq 1998; Holder and Bishnoi 2000).

Stable at accessible pressures and temperatures (e.g., $P > 50$ bar, $T < 7$°C), they occur extensively in permafrost. Furthermore, gas hydrates are found widely on the ocean floors, from the Arctic to the Antarctic, including some tropical seas (but not in the Mediterranean Sea). Their stratigraphy may be easily mapped, due to sharp contrast in acoustic velocities. Sonar investigations show the existence of a layer of gas hydrates and sediments, at depths below 500 m, and several hundred meters thick. This cemented layer contains large reserves of gas hydrate; for instance, the sediments of the Gulf of Cadiz contain 3–16 vol% of gas hydrate.

As a given volume of gas hydrate contains approximately 164 volumes of STP (Standard Temperature and Pressure) methane gas, the methane hydrate behaves as a storage medium, capable of fixing methane in a way similar to compression at 164 bar. Worldwide, clathrates have therefore accumulated an immense amount of methane, estimated to total twice the quantity of carbon present in all the known fossils fuels of the Earth. This raises the possibility of developing technologies to store and transport methane as methane-hydrates, with no necessity of cryogenic refrigeration or high pressure.

As long as they remain stable, gas-hydrates seal the underlying free gas. Consequently, methane hydrates represent a hazard to drillers demanding careful consideration during exploitation (Grauls 2001). Also temperature and/or pressure variations may well destabilize the methane hydrate layer, triggering landslides on the continental slope and even tsunamis (Maslin et al. 2004). Furthermore, the rapid release of methane from frozen gas hydrates has been invoked to explain abrupt climatic inversions from cold to warm periods (Kennett et al. 2002), as the greenhouse gas capacity of methane is 3 to 10 times more effective than carbon dioxide. One more aspect related to destabilization of gas hydrates is the generation of mud volcanoes; in fact, destabilization of gas hydrates would produce mud upwelling and hydrocarbon release.

CONCLUSIONS

Using the IUPAC definition of pore size, the number of examples of natural mesoporous phases does not seem large. For instance, gas hydrates have been included within this review, although they should be more properly included among the microporous ones. Therefore, it is useful to explore briefly the geological, structural and thermodynamic factors determining their occurrence.

Geologically, the limited incidence of mesoporous arrangements reflects the high pressure conditions dominating the solid Earth; namely, the occurrence of any phase with density lower than the average crustal density of 2.6–2.7 g/cm^3 is unlikely. Therefore, this limits the presence of mesoporous phases to the outermost crust, or to very specific environments, such as extensional veins (chrysotile tubes), water-sediment interfaces (clathrates), abrupt high-temperature events (fullerenes), low-pressure extraterrestrial environments.

Structurally, mesoporous arrangements seem to be connected with interactions other than direct chemical bonding among nearest neighbors. For instance, mesoporosity of chrysotile derives from folding and wrapping of a strongly internally connected layer, with only limited layer-to-layer interactions. Similarly, the submesoporous arrangement of gas hydrates is connected with a physical interaction between host and guest species.

Finally, the presence of a stability field for any of the previous mesoporous phases seems dubious, indicating that the formation of these phases may be kinetically controlled rather than thermodynamically stabilized. However, as mineralogical, thermodynamical and geochemical constraints may not hold for man-made materials (at least in the very short time-scale), we may anticipate further future developments in the design, engineering and use of synthetic mesoporous materials.

ACKNOWLEDGMENTS

The author is indebted with Giovanni Ferraris, Emil Makovicky and Tim White, for their careful revisions of an earlier draft.

REFERENCES

Aizenberg J, Black AJ, Whitesides GM (1999) Control of crystal nucleation by patterned self-assembled monolayers. Nature 398:495-498

Ajayan PM, Iijima S (1993) Capillarity-induced filling of carbon nanotubes. Nature 361:333-334

Amelinckx S, Devouard B, Baronnet A (1996) Geometrical aspects of the diffraction space of serpentine rolled microstructures: their study by means of electron diffraction and microscopy. Acta Crystallogr A52: 850-878

Andreani M, Baronnet A, Boullier AM, Gratier JP (2004) A microstructural study of a "crack-seal" type serpentine vein using SEM and TEM techniques. Eur J Mineral 16:585-595
Atkinson RJ (1973) Chrysotile asbestos: colloidal silica surfaces in acidified suspensions. J Colloid Interface Sci 42:624-628
Balan E, Mauri F, Lemaire C, Brouder C, Guyot F, Saitta AM, Devouard B (2002) Multiple-ionic plasmon resonances in naturally occurring multiwall nanotubes: infrared spectra of chrysotile asbestos. Phys Rev Lett 89:177401_1- 177401_4
Ball P (2001) Roll up for the revolution. Nature 414:142-144
Banfield JF, Nealson KH (1997) Geomicrobiology: interactions between microbes and minerals. Rev Mineral 35:1-448
Baronnet A, Belluso E (2002) Microstructures of the silicates: key information about mineral reactions and a link with the Earth and materials sciences. Mineral Mag 66:709-732
Baronnet A, Devouard B (1996) Topology and crystal growth of natural chrysotile and polygonal serpentine. J Cryst Growth 166:952-960
Baronnet A, Mellini M, Devouard B (1994) Sectors in polygonal serpentine, a model based on dislocations. Phys Chem Mineral 21:330-343
Bates TF, Sand LB, Mink JF (1950) Tubular crystals of chrysotile asbestos. Science 111:512-513
Bates TF, Comer JJ (1959) Further observations on the morphology of chrysotile and halloysite. Proceedings of the Sixth National Conference on Clays and Clay Minerals. Pergamon Press, New York p. 237-248
Beyssac O, Rouzaud JN, Goffé B, Chopin C (1994) Graphitization in a high-pressure, low-temperature metamorphic gradient: a Raman microspectroscopy and HRTEM study. Contrib Mineral Petrol 143: 19-31
Bleiman C, Mercier JP (1975) Attaque acide et chloration de l' asbeste chrysotile. Bull Soc Chimie France 3-4:529-534
Bonijoly M, Oberlin M, Oberlin A (1982) A possible mechanism for natural graphite formation. Int J Coal Geol 1:283-312
Bralia A, Ceccherini S, Fratini F, Manganelli Del Fa' C, Mellini M, Sabatini G (1995) Anomalous water absorption in low-grade serpentinites: more water than space? Eur J Mineral 7:205-215
Buseck PR (2002) Geological fullerenes: review and analysis. Earth Planet Sci Lett 203:781-792
Buseck PR, Tsipursky SJ, Hettich R (1992) Fullerenes from the geological environment. Science 257:215-217
Choi I, Smith RW (1972) Kinetic study of dissolution of asbestos fibers in water. J Colloid Interface Sci 40: 253-262
Clifton RA, Huggins JW, Shell HR (1966) Hollow chrysotile fibers. Am Mineral 51:508-511
Cosslett VE, Horne RW (1960) Private communication to Whittaker EJW and Zussman (1971). *In:* Gard JA (1971) The Electron-optical Investigation of Clays. Mineralogical Society Monograph no. 3, p 159-191
Daly TK, Buseck PR, Williams P, Lewis CF (1993) Fullerenese from a fulgurite. Science 259:1599-1601
Dékany I, Turi L, Fonseca A, Nagy JB (1999) The structure of acid treated sepiolites: small angle X-ray scattering and multi MAS-NMR investigations. Appl Clay Sci 14:141-160
Dove PM, De Yoero JJ, Weiner S (2003) Biomineralization. Rev Mineral Geochem 54:1-381
Englezos P (1993) Clathrate hydrates. Ind Eng Chem Res 32:1251-1274
Firouzi A, Monnier A, Bull LM, Besier T, Sieger T, Huo Q, Walker SA, Zasadzinski JA, Glinka C, Nicol J, Margolese D, Stucky GD, Chmelka BF (1995) Cooperative organization of inorganic-surfactant and biomimetic assemblies. Science 267:1138-1143
Ferraris G, Gula A (2005) Polysomatic aspects of microporous minerals –heterophyllosilicates, palysepioles and rhodesite-related structures. Rev Mineral Geochem 57:69-104
Gauthier JP, Caseiro J, Rantsordas S, Bittencourt Rosa D (1995) Nouvelle structure d' empilement compact dans de l' opale noble du Bréil. Compt Rendus Acad Science Paris 320:373-379
Genov G, Kuhs WF, Staykova DK, Goreshnik E, Salamatin AN (2004) Experimental studies on the formation of porous gas hydrates. Am Mineral 89:1228-1239
Graetsch H (1994) Structural characteritics of opaline and microcrystalline silica minerals. Rev Mineral 29: 209-232
Grauls D (2001) Gas hydrates: importance and applications in petroleum exploration. Mar Pet Geol 18:519-523
Grobéty BH, Metraux C, Ulmer P (2004) Chrysotile, a template for metal nanowires. Abstracts volume of the 32nd International Geological Congress, Florence, August 20-28, p 308
Gronow JR (1987) The dissolution of asbestos fibres in water. Clay Minerals 22:21-35
Haq BU (1998) Gas hydrates: greenhouse nightmare? Energy panacea or pipe dream? GSA Today 8:1-6
Harris PJF, Vis RD, Heymann D (2000) Fullerene-like carbon nanostructures in the Allende meteorite. Earth Planet Sci Lett 183:355-359

Hiura H, Ebbesen TW, Fujita J, Tanigaki K, Takada T (1994) Role of sp^3 defects structures in graphite and carbon nanotubes. Nature 367:148-151
Holder GD, Bishnoi PR (2000) Gas hydrates: challenges for the future. Proceedings National Academy of Science, vol. 912, New York, p 1044
Huggins CW, Shell HR (1965) Density of bulk chrysotile and massive serpentine. Am Mineral 50:1058-1067
Iijima S (1991) Helical microtubules of graphitic carbon. Nature 354:56-58
Kennett JP, Cannariato KG, Hendy IL, Behl RJ (2002) Methane hydrates in Quaternary climate change: the clathrate hypothesis. American Geophysical Union, Washington D.C. p 216
Kosuge K, Shimada K, Tsunashima A (1995) Micropore formation by acid treatment of antigorite. Chem Mater 7:2241-2246
Kroto HW, Heath JR, O'Brien SC, Curl RF, Smalley RE (1985) C_{60} backminsterfullerene. Nature 318:162-163
Kuhs WF, Klapproth A, Gotthardt F, Techmer KS, Heinrichs T (2000) The formation of meso- and macroporous gas hydrates. Geophys Res Lett 27:2929-2932
Kuhs WF, Genov G, Staykova D, Zeller A, Techmer KS, Heinrichs T, Bohrmann G (2004) Porous microstructures of gas hydrates. Abstracts Meeting "Micro- and mesoporous mineral phases," Rome 6-7 December 2004, p 103-106
Martinez E, Comer JJ (1964) The concentration and study of the interstitial material in chrysotile asbestos. Am Mineral 49:153-157
Maschmeyer T (1998) Derivatised mesoporous solids. Curr Opin Solid State Mat Sci 3:71-78
Maslin M, Owen M, Say S, Long D (2004) Linking continental-slope failures and climate change: testing the clathrate gun hypothesis. Geology 32:53-56
Mass N, Heylen I, Cool P, Vansant EF (1997) The relation between the synthesis of pillared clays and their resulting porosity. Appl Clay Sci 12:43-60
McCusker LB (2005) IUPAC nomenclature for ordered microporous and mesoporous materials and its application to non-zeolite microporous mineral phases. Rev Mineral Geochem 57:1-16
McCusker LB, Liebau F, Engelhardt G (2001) Nomenclature of structural and compositional characteristics of ordered microporous and mesoporous materials with inorganic hist (IUPAC recommendations 2001). Pure Appl Chem 73:381-394
McCusker LB, Liebau F, Engelhardt G (2001) Nomenclature of structural and compositional characteristics of ordered microporous and mesoporous materials with inorganic hist (IUPAC recommendations 2001). Microporous Mesoporous Mater 58:3-13
McLean RG, Schofield MA, Kean WF, Sommer CV, Robertson DP, Toth D (2001) Botanical iron minerals: correlation between nanocrystal structure and modes of biological self-assembly. Eur J Mineral 13:1235-1242
Mellini M (1986) Chrysotile and polygonal serpentine from the Balangero serpentinite. Mineral Mag 50: 301-306
Monkman LJ (1971) Some chemical and mineralogical aspects of the acid decomposition of chrysotile. Proceedings 2nd International Conference Physics Chemistry Asbestos Minerals, Louvain (Belgium), paper 3-2, p 1-9
Naumann AW, Dresher WH (1996) The influence of sample texture on chrysotile dehydroxylation. Am Mineral 51:1200-1211
Pundsack FL (1955) The properties of asbestos. I. The colloidal and surface chemistry of chrysotile. J Phys Chem 59:892-895
Pundsack FL (1956) The properties of asbestos. II. The density and structure of chrysotile. J Phys Chem 60: 361-364
Pundsack FL (1961) The pore structure of chrysotile asbestos. J Phys Chem 65:30-33
Pundsack FL, Reimschussel G (1956) The properties of asbestos. III. Basicity of chrysotile suspensions. J Phys Chem 60:1218-1222
Regan BC, Aloni S, Ritchie RO, Dahmen U, Zetti A (2004) Carbon nanotubes as nanoscale mass conveyors. Nature 428:924-926
Ripmeester JA, Tse JS, Ratcliffe CI, Powell BM (1987) A new clathrate hydrate structure. Nature 325:135-136
Rossman G (1994) Colored varieties of the silica minerals. Rev Mineral 29:433-468
Rouzaud JN, Clinard C (2002) Quantitative high-resolution transmission electron microscopy: a promising tool for carbon materials characterization. Fuel Proc Technol 77-78:229-235
Rumori C, Mellini M, Viti C (2004) Oriented, not-topotactic olivine > serpentine replacement in mesh-textured, serpentinized peridotites. E J Mineral 16:731-741
Sakamoto Y, Diaz I, Terasaki O, Zhao D, Pérez-Pariente J, Kim JM, Stucky GD (2002). Three-dimensional cubic mesoporous structures of SBA-12 and related materials by electron crystallography. J Phys Chem B 106:3118-3123

Salerno P, Mendioroz S (2002) Preparation of Al-pillared montmorillonite from concentrated dispersions. Appl Clay Science 22:115-123
Sayari A (2003) Mesoporous materials. *In:* The Chemistry of Nanostructured Materials. Yong P (ed) World Scientific Publishing Co., Singapore, p. 39-68
Sharma A, Kyotani T, Tomita A (1999) A new quantitative approach for microstructural analysis of coal char using HRTEM images. Fuel 78:1203-1211
Sloan ED Jr (1998) Clathrate hydrates of natural gases. Marcel Dekker Inc., New York
Sloan ED Jr (2003a) Fundamental principles and applications of natural gas hydrates. Nature 426:353-359
Sloan ED Jr (2003b) Clathrate hydrate measurements: microscopic, mesoscopic, and macroscopic. J Chem Thermodyn 35:41-53
Sloan ED Jr (2004) Introductory overview: hydrate knowledge development. Am Mineral 89:1155-1161.
Soma Y, Seyama H, Soma M (1993) Adsorption of fluorescent dyes to chrysotile asbestos. Clay Science 9: 9-20
Suquet (1989) Effects of dry grinding and leaching on the crystal structure of chrysotile. Clays Clay Mineral 37:439-445
Tartaj P, Cerpa A, Garcia-Gonzalez MT, Serna CJ (2000) Surface instability of serpentine in aqueous suspensions. J Colloid Interface Sci 231:176-181
Titulaer MK, van Miltenburg JC, Jansen JBH, Geus, JW (1993) Characterization of tubular chrysotile by thermoporometry, nitrogen sorption, DRIFTS, and TEM. Clays Clay Mineral 41:496-513
Viti C, Mellini M (1998) Mesh textures and bastites in the Elba retrograde serpentinites. Eur J Mineral 10: 1341-1359
Walsh D, Mann S (1995) Fabrication of hollow porous shells of calcium carbonate from self-organizing media. Nature 377:320-323
White T, Ferraris C, Kim J, Madhavi S (2005) Apatite – an adaptive framework structure. Rev Mineral Geochem 57:307-401
Whittaker EJW (1957) The structure of chrysotile. V. Diffuse reflexions and fibre texture. Acta Cryst 10:149-156
Whittaker EJW (1966) Diffraction contrast in electron microscopy of chrysotile. Acta Cryst 21:461-466
Wicks FJ, O'Hanley DS (1989) Serpentine minerals: structure and petrology. Rev Mineral 19:91-167
Wilson MA, Pang LSK, Vassallo AM (1992) C_{60} separation on coal. Nature 355:117-118
Xia Y, Lu Y, Kamata K, Gates B, Yin Y (2003) Macroporous materials containing three-dimensionally periodic structures. *In:* The Chemistry of Nanostructured Materials. Yong P (ed) World Scientific Publishing Co., Singapore, p 69-100
Yada K (1967) Study of chrysotile asbestos by a high resolution electron microscope. Acta Crystallogr 23: 704-707
Yada K (1971) Study of microstructure of chrysotile asbestos by high resolution electron microscopy. Acta Crystallogr A27:659-664
Yada K, Iishi K (1977) Growth and microstructure of synthetic chrysotile. Am Mineral 62:958-965
Yan H, Yang P (2003) Semiconductor nanowires: functional building blocks for nanotechnology. *In* The Chemistry of nanostructured materials. Yong P (ed) World Scientific Publishing Co., Singapore, p 182-226
Yang H, Coombs N, Ozin GA (1997) Morphogenesis of shapes and surface patterns in mesoporous silica. Nature 386:692-695
Zega TJ, Buseck PR (2003) Fine-grained mineralogy of the Cold Bokkeveld CM chondrite. Geochim Cosmochim Acta 67:1711-1721
Zega TJ, Garvie LAJ, Dodony I, Buseck PR (2004) Serpentine nanotubes in the Mighei CM chondrite. Earth Planet Sci Lett 223:141-146
Zheng N, Bu X, Feng P (2003) Synthetic design of crystalline inorganic chalcogenides exhibiting fast-ion conductivities. Nature 426:428-432